PERGAMON

International Journal of Heat and Mass Transfer 45 (2002) 4599–4606

International Journal of HEAT and MASS TRANSFER

www.elsevier.com/locate/ijhmt

Boiling incipience in microchannels

S.M. Ghiaasiaan *, R.C. Chedester

G.W. Woodruff School of Mechanical Engineering, Georgia Institute of Technology, Atlanta, GA 30332-0405, USA

Received 27 February 2002; received in revised form 22 April 2002

Abstract

The available data dealing with boiling incipience of water in microtubes (tubes with diameters in the 0.1–1 mm range) are analyzed. Macroscale models and correlations appear to under predict the heat fluxes that lead to the boiling incipience in microtubes. It is suggested that boiling incipience in microchannels may be controlled by the thermocapillary force that tends to suppress the microbubbles that form on wall cavities. Accordingly, a semi-empirical method is proposed for predicting the boiling incipience in microtubes. The effect of the turbulence characteristics of the microtube on the proposed method is also examined.
© 2002 Published by Elsevier Science Ltd.

Keywords: Microchannels; Onset of nucleate boiling; Subcooled boiling; Thermocapillary; Turbulence

1. Introduction

Microchannels with hydraulic diameters on the order of 0.1–1 mm have important current and potential applications and their thermal–hydraulic characteristics have been recently studied rather extensively [1]. For single-phase flow different and opposing trends have been reported [2–11]. Among these, the disagreement between measured turbulent flow heat transfer coefficients and the predictions of macroscale correlations can be mentioned [12–15].

Available data dealing with boiling and two-phase flow also suggest important differences between microchannels (defined here as channels for which $D/\lambda \leqslant 0.3$ [1,16]) and commonly applied large channels [1]. In subcooled boiling, the velocity and temperature gradients near the walls of microchannels can be extremely large, rendering forces such as thermocapillary (Marangoni) force and the lift force resulting from the liquid velocity gradient significant, and the released bubbles can be extremely small [17]. The occurrence of extremely small bubbles significantly impacts the various subcooled boiling processes including the onset of nucleate boiling (ONB), onset of significant void (OSV) [18], and departure from nucleate boiling [19]. Experimental data representing ONB and OSV in microtubes, for example show that the widely used macroscale correlations underpredict the heat fluxes that cause both ONB and OSV phenomena in heated microtubes with subcooled water [18].

The objectives of this paper are to show that the observed disagreement between microtube ONB data and macroscale models may be due to the significance of thermocapillary effects in the former, and accordingly develop a semi-analytical model for ONB in microtubes.

2. Microchannel onset of nucleate boiling data

In forced-flow subcooled boiling, the boiling incipience, or the ONB point, represents the initiation of nucleate boiling, and can be specified in macroscale experiments by photographic methods. This technique can be easily applied to microchannels, and instead the heated channel pressure drop–mass flux (ΔP–G) characteristic curve can be used for the specification of the ONB and OSV points [18,20]. The general form of the ΔP–G curve, obtained by measuring the total pressure drop across a test section subject to a constant thermal load and a variable subcooled coolant mass flux (e.g., water at

* Corresponding author. Tel.: +1-404-894-3746; fax: +1-404-894-8496.

E-mail address: seyed.ghiaasiaan@me.gatech.edu (S.M. Ghiaasiaan).

0017-9310/02/$ - see front matter © 2002 Published by Elsevier Science Ltd.
PII: S0017-9310(02)00167-9

Nomenclature

a, b	empirical coefficients
B	constant in the logarithmic velocity distribution
C	empirical coefficient
D	channel diameter (m)
f	D'Arcy friction factor
F_σ	thermocapillary force (N)
G	mass flux (kg/m^2 s)
h	convection heat transfer coefficient (W/m^2 K)
h_{fg}	latent heat of vaporization (J/kg)
k	thermal conductivity (W/m K)
l	length scale defined in Eq. (17)
Nu	Nusselt number $= hD/k$
Nv	Ohnesorge number
P	pressure (Pa)
Pe	Peclet number $= \overline{U}D/\alpha$
Pr	Prandtl number $= v/\alpha$
q''	heat flux (W/m^2)
r	radial coordinate (m)
R	channel radius (m)
R^*	critical cavity radius (m)
Re	Reynolds number $= \overline{U}D/v$
T	temperature (K)
$\overline{T}$	liquid bulk temperature (K)
u	velocity (m/s)
$\overline{U}$	channel average velocity (m/s)
u^*	friction velocity $= \sqrt{\tau_w/\rho}$ (m/s)
v	specific volume (m^3/kg)
v_{fg}	$v_g - v_f$
u^+	dimensionless velocity $= u/u^*$
y	distance from the wall (m)
y_B	height of bubble tip above the wall surface (m)
y_n^+	parameter in Reichardt's eddy diffusivity model

Greek symbols

ε_H	heat transfer eddy diffusivity (m^2/s)
ε_M	momentum eddy diffusivity (m^2/s)
κ	Karman's constant
λ	Laplace length scale $= \sqrt{\sigma/g(\rho_l - \rho_g)}$ (m)
v	kinematic viscosity (m^2/s)
θ	azimuthal angle (R)
ρ	density (kg/m^3)
σ	surface tension (N/m)
τ	shear stress (Pa)
ξ	dimensionless parameter defined in Eq. (14)

Subscripts

B	bubble
exp	experiment
f	saturated liquid
I	bubble–liquid interface
mod	model
sat	saturation
w	wall

Superscripts

+	in wall units

Acronyms

OFI	onset of flow instability
ONB	onset of nucleate boiling
OSV	onset of significant void

low and moderate pressures) with invariant inlet temperature, is depicted in Fig. 1 [21]. By comparing the calculated single-phase liquid pressure drop line with the ΔP–G curve, the ONB point can be identified as the point where the latter two lines begin to deviate noticeably. This method has been used by Inasaka et al. [20] and Kennedy et al. [18]. An audible, whistle-like sound accompanied the occurrence of ONB in the experiments of Kennedy et al. [18], further confirming the reliability of the aforementioned method for the specification of the ONB point. The data of [20] obtained with their 1 mm diameter test section, and the data of [18] obtained with their 1.17 and 1.45 mm diameter test sections, are depicted in Fig. 2(a) and (b). In the figures they are compared with the predictions of the widely used macroscale correlations of Bergles and Rosenow [22] and Sato and Matsumura [23]; the latter correlation is identical to the correlation of Davis and Anderson for hemispherical

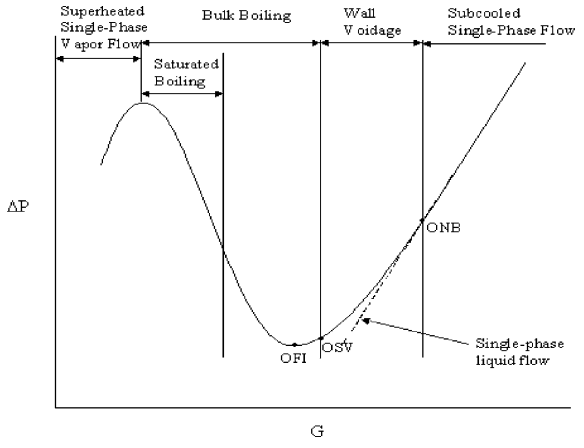

Fig. 1. Pressure drop–mass flux characteristic curve for a uniformly heated channel.

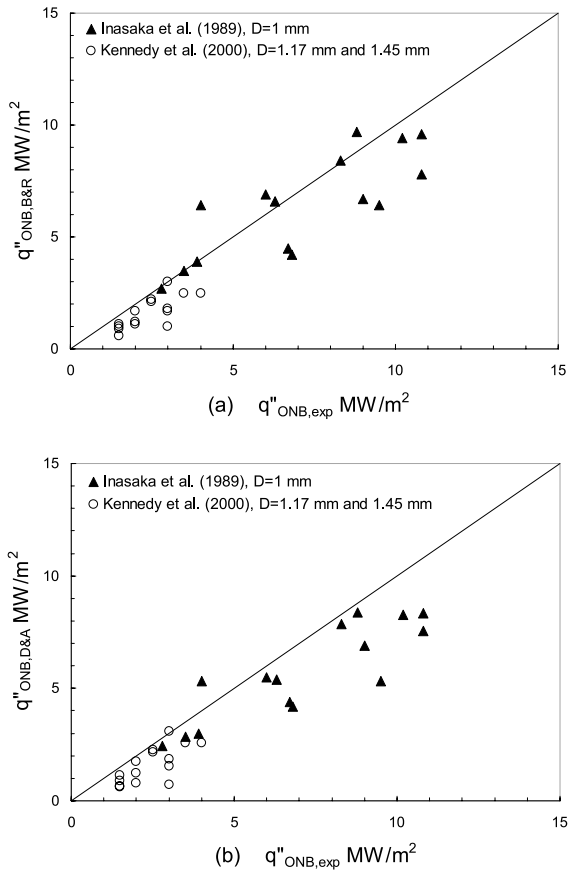

Fig. 2. Comparison between the microtube ONB data and two widely used macroscale models. (a) Bergles and Rohsenow [22] (b) Sato and Matsumura [23].

bubbles [24]. (Both correlations are described in the next section.) The depicted predictions of these correlations were obtained by applying the Dittus–Boelter correlation for forced convection, as described later. Overall, both correlations evidently under predict q''_{ONB} in the described experiments.

3. Past onset of nucleate boiling models

Several models have been proposed for boiling incipience for partially wetting liquid–solid systems [22–28], and for highly wetting liquids [29,30]. For the partially wetting conditions, all of the aforementioned models are based on the tangency criterion. The bubbles are assumed to grow on cavities of various sizes in a superheated liquid layer with a linear temperature profile, and ONB is assumed to occur when the following conditions apply to any of the bubbles:

$$T|_{y=y_{\mathrm{B}}} = T_{\mathrm{B}} \tag{1}$$

$$\frac{\partial T}{\partial y}|_{y=y_{\mathrm{B}}} = \frac{\partial T_{\mathrm{B}}}{\partial R_{\mathrm{B}}} \tag{2}$$

where $\partial T_{\mathrm{B}}/\partial R_{\mathrm{B}}$ is obtained using some form of the Clausius–Clapeyron's relation. Properties without a subscript everywhere in the paper represent the liquid phase. The method of Bergles and Rohsenow [22] is the most widely used, and for water its predictions have been correlated as [22]:

$$q''_{\mathrm{ONB}} = 5.30P^{1.156}\left[1.8(T_{\mathrm{w}} - T_{\mathrm{sat}})_{\mathrm{ONB}}\right]^{n} \tag{3}$$

where $n = 2.41/P^{0.0234}$. Here q''_{ONB} is in W/m^2, P is in kPa, and temperatures are in K. The model of Davis and Anderson [24] considers chopped-spherical bubbles, and for hemispherical bubbles gives the following expression with $C = 1$; in agreement with [23]:

$$q''_{\mathrm{ONB}} = \frac{k_{\mathrm{f}} h_{\mathrm{fg}}}{C(8\sigma T_{\mathrm{sat}} \mathbf{v}_{\mathrm{fg}})}(T_{\mathrm{w}} - T_{\mathrm{sat}})^2 \tag{4}$$

Expressions similar to the above equations should of course be used simultaneously with an equation for the convection heat transfer:

$$q''_{\mathrm{ONB}} = h(T_{\mathrm{w}} - \overline{T}) \tag{5}$$

The heat transfer coefficient is usually obtained from widely used correlations such as [31,32]. The adequacy of these correlations for microchannels is questionable, however [9–14], and they appear to systematically underpredict h for heated microtubes [1–3,15]. Marsh and Mudawar [28] investigated the ONB in subcooled turbulent liquid falling films, and noted that the assumption of linear liquid temperature profile near the wall was inadequate. Due to the complicating effects of the bubble on its surrounding liquid isotherms and the turbulent eddies that may suppress nucleation, however, they correlated their data semi-empirically, and derived an expression similar to Eq. (4), with $C = 3.5$.

It should be mentioned that the aforementioned models all assume the occurrence of an essentially stationary bubble layer on the wall cavities at the vicinity of the ONB point. Recent studies dealing with bubble ebullition phenomena in subcooled boiling, using water at low pressure, have shown that bubbles slide along the heated surface near the ONB point, before being ejected [33,34]. Furthermore, the released bubble diameters predicted by the commonly applied macroscale models for microchannels are sufficiently small to render the relative magnitudes of forces that act on bubbles different from macroscale cases [17].

4. Fully turbulent flow in a microtube

The wall heat transfer coefficient is needed for the application of most ONB models, including the model

presented in this paper. For incompressible, fully developed and constant property flow in a circular tube:

$$Re = \frac{\overline{U}D}{v} = 4\int_0^{R^+} u^+ \mathrm{d}y^+ - \frac{4}{R^+}\int_0^{R^+} u^+ y^+ \mathrm{d}y^+ \tag{6}$$

where $y^+ = yu^*/v$; $u^+ = u/u^*$; and

$$u^* = \sqrt{\tau_w/\rho} = \overline{U}\sqrt{f/8} = 2\frac{R^+\overline{U}}{Re} \tag{7}$$

For smooth, circular tubes the fully developed turbulent velocity profile obeys the well-known law of the wall distribution with $\kappa = 0.4$ and $B = 5.5$ [35,36]. Surface roughness and particles, furthermore, modify the velocity profile. The channel convection heat transfer coefficient depends on the turbulent velocity profile according to [38]:

$$\frac{k}{hD} = \frac{1}{Nu} = \frac{2}{\left(\overline{U}^+ R^{+2}\right)^2} \times \int_0^{R^+} \left\{ \left(\int_0^{r^+} u^+ r^+ \mathrm{d}r^+ \right)^2 \left[\left(1 + \left(\frac{\varepsilon_H}{\varepsilon_M} \right) \mathrm{Pr} \frac{\varepsilon_M}{v} \right) r^+ \right]^{-1} \right\} \mathrm{d}r^+ \tag{8}$$

where

$$u^+ = \frac{1}{R^+}\int_{r^+}^{R^+} \frac{r^+ \mathrm{d}r^+}{1 + \varepsilon_M/v} \tag{9}$$

Using the above equations along with an appropriate eddy diffusivity model, the velocity profile and heat transfer coefficient in the channel can be calculated. A well-proven expression for eddy diffusivity in tubes is [38]:

$$\varepsilon_M/v = \kappa\left\{ y^+ - y_n^+ \tanh(y^+/y_n^+) \right\} \tag{10}$$

for $y^+ \leqslant 50$, and

$$\varepsilon_M/v = (\kappa/3) y^+ \left\{ 0.5 + (r^+/R^+)^2 \right\} (1 + r^+/R^+) \tag{11}$$

for $y^+ > 50$, where $\kappa = 0.4$ and $y_n^+ = 11$.

The above equations were used for calculating and correlating wall heat transfer coefficient and friction factor by Petukhov [37], who also derived simple methods for the effect of the liquid property variations with temperature. The microtube forced-convection heat transfer data of [9,10] could also be predicted by the above equations when the parameters in the Reichardt eddy diffusivity model [38] are modified [15].

5. The present model for onset of nucleate boiling

Hemispherical bubbles of various sizes are assumed to form on the wall cavities, and Eq. (1), with $y_B = R_B$, is maintained as a requirement for the occurrence of the bubble. It is, however, hypothesized that ONB occurs in a microtube when the suppressing effect of the thermocapillary force acting on some bubbles is balanced by the aerodynamic force on those bubbles. Assuming that the bubble size is negligibly small compared with channel radius, the thermocapillary force for a hemispherical bubble can be represented as:

$$F_\sigma = 2\pi R_B^2 \int_0^{\pi/2} \left[(\partial\sigma/\partial T)(\partial T_I/\partial y) \right]_{y = R_B \cos\theta} \sin^2\theta \, \mathrm{d}\theta \tag{12}$$

where θ is the hemisphere's azimuthal angle, and y is the coordinate perpendicular to the surface. The interfacial temperature is likely to be slightly non-uniform [39,40], however, and when the liquid–vapor surface tension decreases with increasing temperature, F_σ will tend to slightly deform the bubble [41]. The aerodynamic force also depends on the fluid motion around the bubble surface. Rigorous modeling is difficult, however, due to the complicating mutual effects of the bubble and the surrounding flow field, and the turbulent eddies that penetrate the near-wall fluid layer [28]. A semi-empirical analysis is therefore performed. The ratio between the orders of magnitude of the thermocapillary and aerodynamic forces is simply represented by the following dimensionless quantity:

$$\xi = \frac{\sigma_f - \sigma_w}{\rho_f \overline{U}^2 R^*} \tag{13}$$

where σ_f and σ_w are the values of the surface tension at T_{sat} and T_w respectively, and R^* is the critical cavity radius that satisfies Eqs. (1) and (2) when the surrounding liquid temperature is linearly distributed with respect to y:

$$R^* = \left[\frac{2\sigma T_{sat} \mathbf{v}_{fg} k_f}{q''_{ONB} h_{fg}} \right]^{1/2} \tag{14}$$

Following [28], Eq. (4) is used as the basis for the development of a semi-empirical correlation, and in light of the above discussion, the coefficient C is expected to be a strong function of ξ in microchannels.

Fig. 3 displays the experimental values of C as a function of parameter ξ for the microchannel ONB data of [18,20]. These values of C were obtained as follows. First, for each data point, knowing the experimental mass flux, wall heat flux, $q''_{ONB,exp}$, and local liquid bulk temperature, $\overline{T}$, at the ONB point, the heat transfer coefficient and the turbulent velocity distribution in the microtube were obtained, following the procedure detailed in [15]. Briefly, this was done by solving Eqs. (6)–(11) assuming $\kappa = 0.4$ and $y_n^+ = 11$, using 1800 radial nodes, with 1000 equal-sized nodes representing the $1 > r/R \geqslant 0.85$ region of the tube cross-section, and 800 equal-sized nodes representing the remainder of the tube cross-section. Parameter R^* was then calculated from Eq. (14) with σ representing saturated liquid, followed

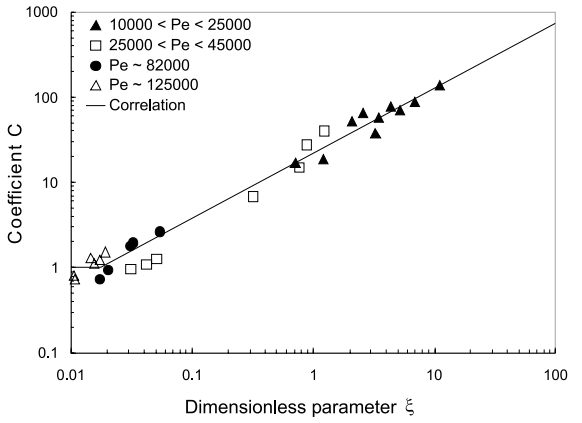

Fig. 3. Variations of coefficient C as a function of the dimensionless parameter ξ ($\kappa = 0.4$, $y_n^+ = 11$).

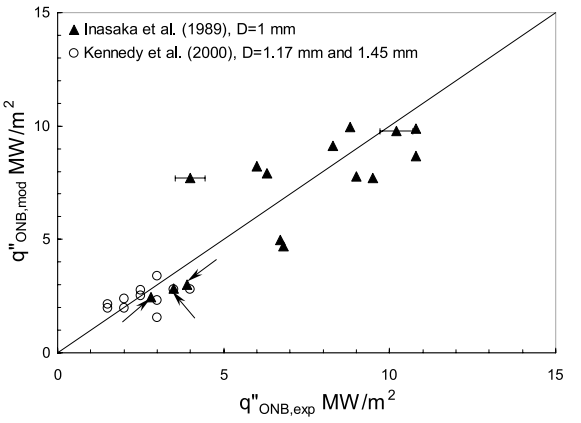

Fig. 4. Comparison of microtube ONB data with the predictions of the present model ($\kappa = 0.4$, $y_n^+ = 11$). Points designated with arrows were obtained with $C = 1$.

by the calculation of ξ from Eq. (13). Fig. 3 confirms a strong dependence of C on ξ, with C monotonically increasing (equivalent to a monotonically increasing q''_{ONB} for given local coolant conditions) as ξ is increased. Increasing ξ of course implies stronger suppression of bubbles by the thermocapillary force. Fig. 3 also indicates that C is independent of Pe, as expected. The dependence of C on ξ in Fig. 3 can be represented by the following simple correlation:

$$C = a\xi^b \tag{15}$$

with the limit of:

$$C \geqslant 1 \tag{16}$$

The constants in Eq. (15) are $a = 22$ and $b = 0.765$. The limit in Eq. (16) is only marginally supported by the data, and is imposed since, as $\xi \to 0$, the thermocapillary force tends to vanish, and the macroscale correlations of [23,24] (the latter for assumed hemispherical bubbles) should apply. The predictions of the present model for ONB are now depicted in Fig. 4, where they are compared with the data of [18,20]. These model calculations were obtained by solving Eqs. (6)–(11), along with Eqs. (13)–(16). Physically correct, converged solutions were easily obtained for all data points, except for three data points of [20], which are designated with arrows in the figure. These and all other parametric calculation, however, show that difficulty with convergence is encountered only in some cases for which $C \approx 1$, and for such cases good prediction of data can be obtained by simply assuming $C = 1$, in agreement with the correlations of [23,24]. The range of the experimental parameters for the above model are: $10{,}000 < Pe < 125{,}000$; $0.01 < \xi < 11$; and $95{,}000 < D/l < 750{,}000$, where l represents a length scale that can be derived based on dimensional analysis using liquid properties but excluding gravity due to the negligible effect of buoyancy on two-phase flow phenomena in microchannels [41]:

$$l = \rho v^2/\sigma \tag{17}$$

Definition of l is consistent with the way a surface tension parameter is defined when a strong dependence of the latter parameter on the velocity or rate of shear is avoided. By dividing l by a relevant geometric length (e.g., R), one obtains Nv^2, where Nv is the Ohnesorge or viscosity number, which plays an important role in droplet breakup [42,43]. Nv^2 can also be interpreted as a surface tension parameter that does not depend on velocity [44]. The mean and standard deviation of the statistic $(1 - q''_{\mathrm{ONB}}/q''_{\mathrm{ONB,exp}})$ are 0.229 and 0.185, respectively. The large standard deviation, it should be mentioned, is due to the data scatter.

Some parametric calculation results are displayed in Fig. 5, where the effects of channel diameter, liquid subcooling, and Pe on q''_{ONB} are examined, using water at

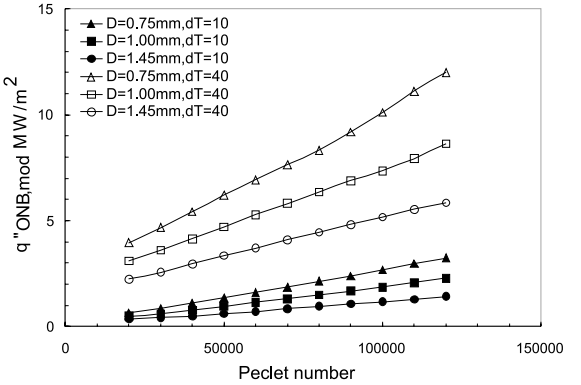

Fig. 5. Some parametric calculations for water in a tube with $D = 1.00$ mm and $P = 10$ atm.

10 bar pressure as the working fluid and the experimental system of [18] as the basis. According to the model, q''_{ONB} monotonically increases with increasing Pe and subcooling, as expected. The model also predicts a strong dependence of q''_{ONB} on channel diameter. The latter parametric dependence of course needs experimental verification, in particular for channels significantly smaller in diameter than 1 mm.

6. Effect of channel turbulence characteristics

The calculations described in the previous section were repeated in order to examine the effect of channel turbulence characteristics on the developed model parameters. As noted earlier, the liquid forced convection data of [9,10] are well predicted by Eqs. (8)–(11), with proper adjustments of parameters κ and y_n^+. In order to examine the sensitivity of the proposed model to channel turbulence characteristics, the analysis is repeated in this section using the adjusted values of the aforementioned parameters based on the data of [9,10].

Figs. 6 and 7 are similar to Figs. 3 and 4, respectively, with the difference that the former figures were obtained by assuming $\kappa = 0.4$ and $y_n^+ = 8.5$ for the eddy diffusivity model of Reichardt [39] (Eqs. (10) and (11)), consistent with the observations in [15]. The reduction of the value y_n^+ while κ remains unchanged implies stronger damping of turbulence in the near wall zone. With the aforementioned turbulence characteristics, the constants in Eq. (15) had to be replaced with: $a = 12$ and $b = 0.721$. The mean and standard deviation of the statistic $(1 - q''_{ONB}/q''_{ONB,exp})$ are 0.223 and 0.189, respectively.

Alternatively, by assuming that $\kappa = 0.48$ and $y_n^+ = 11$ [15], the data could be correlated by Eq. (15) with $a = 13$ and $b = 0.738$. Increasing κ in Reichhardt's eddy diffusivity model while y_n^+ remains unchanged implies stronger turbulence energy transport in the channel core. For this case, the mean and standard deviation of the aforementioned statistic are 0.214 and 0.183, respectively.

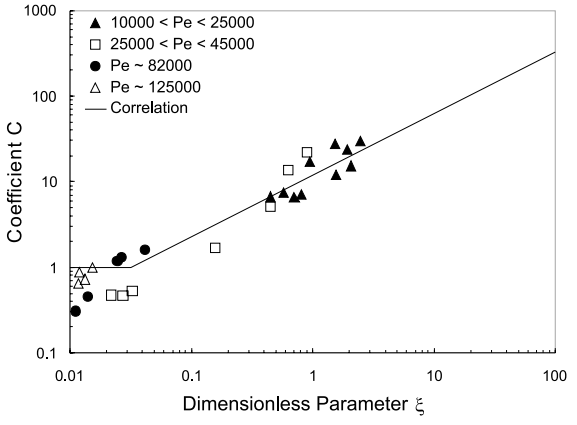

Fig. 6. Variations of coefficient C as a function of the dimensionless parameter ξ ($\kappa = 0.4$, $y_n^+ = 8.5$).

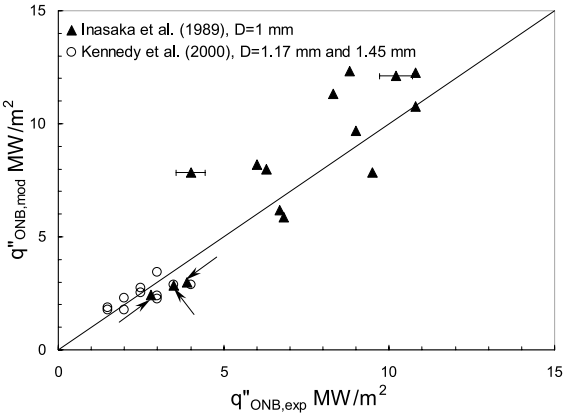

Fig. 7. Comparison of microtube ONB data with the predictions of the present model ($\kappa = 0.4$, $y_n^+ = 8.5$). Points designated with arrows were obtained with $C = 1$.

The constants in the correlation developed for the prediction of ONB in this work evidently depend on the microtube turbulence characteristics, and when the eddy diffusivity profile is assumed to be similar to the macroscale case, Eq. (15) is recommended. These results, nevertheless, confirm the need for the elucidation of the causes for the observed differences between turbulent flows in micro and large systems.

7. Concluding remarks

A semi-empirical method for the calculation of the boiling incipience heat flux in water-cooled microtubes was developed in this paper, based on the available data. The method is based on the hypothesis that in microchannels the thermocapillary force which tends to suppress the microbubbles that form on wall cavities plays a crucial role. The correlation parameters were shown to depend on the turbulence characteristics of the microtube.

References

[1] S.M. Ghiaasiaan, S.I. Abdel-Khalik, Two-phase flow in microchannels, Progr. Heat Transfer 34 (2001) 145–254.

[2] E.P. Mikol, Adiabatic single and two-phase flow in small bore tubes, ASHRAE J. 5 (1963) 75–86.

[3] R. Acosta, R. Muller, C. Tobins, Transport processes in narrow (capillary) channels, AIChE J. 31 (1985) 473–482.
[4] W. Tong, A.E. Bergles, M.K. Jensen, Pressure drop with highly subcooled flow boiling in small-diameter tubes, Exp. Thermal Fluid Sci. 15 (1997) 202–212.
[5] C.-O. Olson, B. Sunden, Pressure drop characteristics of small-sized tubes, ASME paper no. 94-WA/HT-1, Presented at the 1994 Winter Annual Meeting.
[6] R.S. Stanley, R.F. Barron, T.A. Ameel, Two-phase flow in microchannels, ASME DSC-62/HTD-354, 1997 pp. 143–152.
[7] S.B. Choi, R.F. Barron, R.O. Warrington, Fluid flow and heat transfer in microtubes, ASME DSC-32 (1991) 123–134.
[8] W. Yu, R.O. Warrington, R.F. Barron, T.A. Ameel, An experimental and theoretical investigation of fluid flow and heat transfer in microtubes, Proc. ASME/JSME Thermal Eng. Conference 1 (1995) 523–530.
[9] T.A. Adams, S.I. Abdel-Khalik, S.M. Jeter, Z. Qureshi, An experimental investigation of single-phase forced convection in microchannels, Int. J. Heat Mass Transfer 41 (1997) 851–859.
[10] T.A. Adams, S.M. Ghiaasiaan, S.I. Abdel-Khalik, Enhancement of liquid forced convection heat transfer in microchannels due to the release of dissolved noncondensables, Int. J. Heat Mass Transfer 42 (1999) 3563–3573.
[11] X.F. Peng, B.-X. Wang, Liquid flow and heat transfer in microchannels with and without phase change, Proc. 10th Int. Heat Transfer Conference 1 (1994) 159–177.
[12] X.F. Peng, B.-X. Wang, G.P. Peterson, H.P. Ma, Experimental investigation of heat transfer in flat plates with rectangular microchannels, Int. J. Heat Mass Transfer 38 (1995) 127–137.
[13] B.-X. Wang, X.F. Peng, Experimental investigation of liquid forced-convection heat transfer through microchannels, Int. J. Heat Mass Transfer 37 (1994) 73–82.
[14] X.F. Peng, G.P. Peterson, The effect of thermofluid and geometrical parameters on convection of liquids through rectangular microchannels, Int. J. Heat Mass Transfer 38 (1995) 755–758.
[15] S.M. Ghiaasiaan, T.S. Laker, Turbulent forced convection in microtubes, Int. J. Heat Mass Transfer 44 (2001) 2777–2782.
[16] M. Suo, P. Griffith, Two-phase flow in capillary tubes, J. Basic Eng. 10 (Part 2) (1964) 166–185.
[17] C.L. Vandervort, A.E. Bergles, M.K. Jensen, Heat transfer mechanisms in very high heat flux subcooled boiling, ASME Fundamentals of Subcooled Flow Boiling, HTD 217 (1992) 1–9.
[18] J.E. Kennedy, G.M. Roach Jr., M.E. Dowling, S.I. Abdel-Khalik, S.M. Ghiaasiaan, S.M. Jeter, Z.H. Qureshi, The onset of flow instability in uniformly heated horizontal microchannels, ASME J. Heat Transfer 122 (2000) 118–125.
[19] G.P. Celata, M. Cumo, A. Mariani, H. Nariai, F. Inasaka, Influence of channel diameter on subcooled flow boiling burnout at high heat fluxes, Int. J. Heat Mass Transfer 44 (1993) 3407–3409.
[20] F. Inasaka, H. Nariai, T. Shimura, Pressure drop in subcooled boiling in narrow tubes, Heat Transfer—Jpn. Res. 18 (1989) 70–82.
[21] G. Yadigaroglu, Two-phase flow instabilities and propagation phenomena, in: Thermohydraulics of Two-phase Systems for Industrial Design and Nuclear Engineering, Hemisphere, Washington DC, 1981, pp. 353–403.
[22] A.E. Bergles, W.M. Rohsenow, The determination of forced-convection Surface boiling heat transfer, ASME J. Heat Transfer C 86 (1964) 365–372.
[23] T. Sato, H. Matsumura, On the conditions of incipient subcooled boiling and forced convection, Bull. Jpn. Soc. Mech. Eng. 7 (1963) 392–398.
[24] E.J. Davis, G.H. Anderson, The incipience of nucleate boiling in forced convection flow, AIChE J. 12 (1966) 774–780.
[25] C.V. Han, P. Griffith, The mechanism of heat transfer in nucleate pool boiling—I. Bubble initiation, growth and departure, Int. J. Heat Mass Transfer 8 (1965) 887–904.
[26] S.T. Yin, A.H. Abdelmessih, Prediction of incipient flow boiling from a uniformly heated surface, AIChE Symp. Series 164 (1974) 236–243.
[27] Y. Sudo, K. Miyata, K.H. Ikawa, M. Kaminaga, Experimental study of incipient nucleate boiling in narrow vertical rectangular channel simulating subchannel of upgraded JRR-3, J. Nucl. Sci. Technol. 23 (1968) 73–82.
[28] W.J. Marsh, I. Mudawar, Predicting the onset of nucleate boiling in wavy free-falling turbulent liquid films, Int. J. Heat Mass Transfer 32 (1989) 361–378.
[29] W. Tong, A. Bar-Cohen, T.W. Simon, S.M. You, Contact angle effects on boiling incipience of highly wetting liquids, Int. J. Heat Mass Transfer 33 (1990) 91–103.
[30] S.M. You, T.W. Simon, A. Bar-Cohen, W. Tong, Experimental investigation of nucleate boiling incipience with a highly wetting dielectric fluid (R-113), Int. J. Heat Mass Transfer 33 (1990) 105–117.
[31] F.W. Dittus, L.M.K. Boelter, Heat transfer in automobile radiators of tubular type, University of California Publ. Eng. 2 (1930) 443–461.
[32] E.N. Sieder, G.E. Tate, Heat transfer and pressure drop of liquids in tubes, Ind. Eng. Chem. 28 (1936) 1429–1439.
[33] E.L. Bibeau, M. Salcudeau, Subcooled void growth mechanisms and prediction at low pressure and low velocity, Int. J. Multiphase Flow 20 (1994) 837–863.
[34] E.L. Bibeau, M. Salcudeau, A study of bubble ebullition in forced-convective subcooled nucleate boiling at low pressure, Int. J. Heat Mass Transfer 37 (1994) 2245–2259.
[35] T. Von Karman, The analogy between fluid friction and heat transfer, Trans. ASME (1939) 705.
[36] H. Schlichting, Boundary-Layer Theory, McGraw-Hill, New York, 1968.
[37] B.S. Petukhov, Heat transfer and friction in turbulent pipe flow with variable physical properties, Adv. Heat Transfer 6 (1970) 503–565.
[38] H. Reichardt, Die Grundlagen des turbulent warmeuberganges, Arch. Ges. Warmetech 2 (1951) 129–142.
[39] R. Marek, J. Straub, The origin of thermocapillary convection in subcooled nucleate pool boiling, Int. J. Heat Mass Transfer 44 (2001) 619–632.

[40] A.K. Akbar, R.C. Chedester, S.M. Ghiaasiaan, Thermocapillary effects in heterogeneously formed bubbles in microsystems, to be presented at IMECE-2002, New Orleans, LA, November 2002.
[41] R.C. Chedester, S.M. Ghiaasiaan, A proposed mechanism for hydrodynamically controlled onset of significant void in microtubes, Int. J. Heat Fluid Flow, in press.
[42] O.J. Hinze, Fundamentals of the hydrodynamic mechanism of splitting in dispersion process, AIChE J. 1 (1955) 289–295.
[43] R.D. Cohen, Effect of viscosity on drop breakup, Int. J. Multiphase Flow 20 (1994) 211–216.
[44] L. Preziosi, K. Chen, D.D. Joseph, Lubricated pipelining: stability of core-annular flow, J. Fluid Mech. 201 (1989) 325–356.